Conformational Dynamics of the Estrogen Receptor α: Molecular Dynamics Simulations of the Influence of Binding Site Structure on Protein Dynamics†

Leyla Celik,‡ Julie Davey Dalsgaard Lund,§ and Birgit Schiøtt*,‡,§

Interdisciplinary Nanoscience Centre (iNANO) and Centre for Insoluble Protein Structures (inSPIN), Department of Chemistry, University of Aarhus, DK-8000 Aarhus C, Denmark

Received August 15, 2006; Revised Manuscript Received November 24, 2006

ABSTRACT: We present 158 ns of unrestrained all-atom molecular dynamics (MD) simulations of the human estrogen receptor α ligand binding domain (ERα LBD) sampling the conformational changes upon binding of estradiol. The pivotal role of His524 in maintaining the protein structure in the biologically active agonist conformation is elucidated. With His524 modeled as the ϵ-tautomer, a conserved hydrogen bond to the ligand is found in the active complex. Helices 3 and 11 are held together by a hydrogen-bonding network from His524 to Glu339 via Glu419 and Lys531, arresting the ligand in the binding pocket and creating the "mouse trap" binding site for helix 12 (H12). The simulations reveal how His524 serves as a communication point between the two. When estradiol is bound, His524 is positioned correctly for the hydrogen bond network to be established. H12 is then positioned for interaction with the co-activator protein, leading to the biologically active complex. The conformational dynamics of ERα LBD is further investigated from simulations of antagonist and apo conformations of the protein. These simulations suggest a likely sequence of events for the transition from the inactive apo structure to the transcriptionally active conformation of ERα LBD. Stable conformations are identified where H12 is placed neither in the "mouse trap" nor in the co-activator binding groove, as is the case for antagonist structures of ERα LBD. Finally, the influence of such conformations on the biological function of ERα is discussed in relationship to the interaction with selective estrogen receptor modulators and endocrine-disrupting compounds.

The estrogen receptor (ER[1]) is a member of the nuclear receptor (NR) superfamily (*1*, *2*). These proteins are ligand activated transcription factors involved in a number of biological processes, such as homeostasis, lipid metabolism, embryonic development, and cell death (*1*, *3*−*7*). Upon the dysfunction of NRs, diseases and malfunctions, such as obesity, diabetes, infertility, and cancer, may develop (*4*, *5*, *8*). The NR family consists of 48 different proteins (*2*, *9*), each consisting of three functional domains (*10*). These are the N-terminal transactivation domain, the central DNA binding domain, and the C-terminal ligand binding domain (LBD), where the activation function-2 (AF-2) is positioned. The overall architecture of the LBD is conserved among all NRs (*11*); however, selective ligand interactions are entirely due to this domain. Various isoforms of NR LBDs, all with their own particular ligand specificity, may be found in different tissues and thus provide opportunities for specific medicinal targeting of these domains. Apart from ligand binding, the NR LBD is involved in receptor dimerization and is additionally crucial for the binding of cofactors that are important for correct transcriptional interaction (*3*). Upon activation of the ER, a major conformational change takes place in the LBD, where the C-terminal helix, helix 12 (H12), is repositioned to either cap the ligand binding site, in what has been termed the "mouse trap" (*7*), as for the agonist protein structures, or to reside in the so-called "charge clamp" site (*12*) in the antagonist protein structure. When H12 is positioned in the agonist position, a co-activator protein, with a common LXXLL motif (*13*), is bound. These proteins are important for activity because the homo-dimerization of ERα LBD is induced upon this coordination (*14*), allowing the transcription to take place. When an antagonist ligand binds in the ligand binding cavity, however, H12 occupies the surface area where the co-activator protein should bind, thus preventing dimerization and transcription from occurring. In this conformation, ER instead recruits co-repressor proteins (*15*).

No 3D structure has yet been obtained of an entire NR with all domains intact, indicating an overall non-globular protein. Rather, the three functional domains may be thought of as separate pearls on a string. However, 3D structures of the DNA binding domain (*16*−*18*) and the LBD (*3*) alone of several human NRs have been solved during the past decade, revealing that all NR LBDs share an overall common fold that primarily consists of α-helices. The first X-ray

† This work was supported by the Danish Natural Science Foundation, the Carlsberg Foundation, and the Danish Research Foundation as well as the Interdisciplinary Nanoscience Centre, *i*NANO.

* To whom correspondence should be addressed. Phone: +45 8942 3953. Fax: +45 8619 6199. E-mail: birgit@chem.au.dk.

‡ Interdisciplinary Nanoscience Centre.

§ Centre for Insoluble Protein Structures.

[1] Abbreviations: ER, estrogen receptor; hER, human ER; NR, nuclear receptor; LBD, ligand binding domain; RAR, retinoic acid receptor; E2, estradiol; copep, co-activator peptide with sequence NAL***LRYLL***D; AF-2, activation function-2; RMSD, root-mean-square deviation; MD, molecular dynamics; OHT, 4-hydroxytamoxifen; RAL, raloxifen; H, helix; DDE, dichorodiphenyldichloroethylene; DDT, dichlorodiphenyltrichloroethane; PPAR, peroxisome proliferator-activated receptor; TR, thyroid receptor.

10.1021/bi061656t CCC: $37.00
Published on Web 01/24/2007

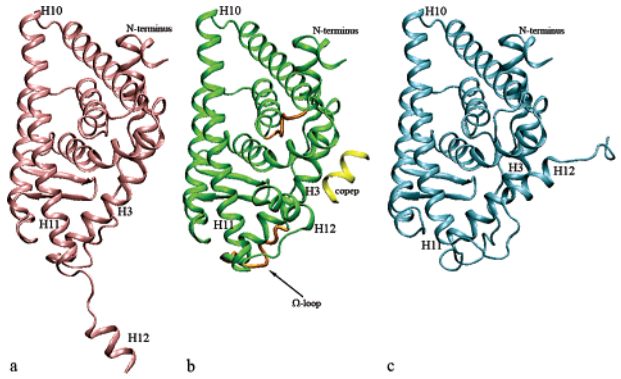

FIGURE 1: (a) Backbone of apo (pink) (*20*), (b) agonist (green) with the cocrystallized copep (yellow) and missing loops (orange) included (*21*), and (c) antagonist (cyan) (*22*) conformations of hERα LBD aligned by structure. Important helices are labeled.

Scheme 1: Molecular Structures of Selected ERα Ligands

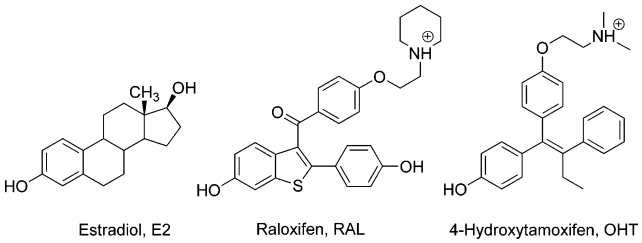

structure of the α isoform of the human ER LBD was solved in 1997 (*19*). Since then, more than 20 different 3D protein structures have been solved of the hERα LBD. Upon comparison of all 3D structures of the LBD of NRs, it becomes obvious that (at least) three different structural conformations are found for the protein, as displayed in Figure 1 for hERα; an apo conformation (*20*), where H12 is extending away from the core of the LBD, an agonist conformation (*21*), which becomes the transcriptional active conformation of the protein upon the binding of co-activators, and finally an antagonist conformation with H12 resting in the co-activator binding pocket (*22*). This nomenclature refers to the overall fold of the domain, especially to the position of H12, but does not refer to what may be captured in the ligand binding pocket. The agonist conformation of NR LBDs always has the same tertiary structure and is often captured with a fragment of the co-activator protein, whereas several apo and antagonist conformations are found (*23*, *24*). All conformations share a certain similarity of the binding site region composed of amino acids from helices 3, 4, 6, 8, and 11. Three residues are particularly important for ligand binding in ERα LBD, namely, Glu353, Arg394, and His524. These are the only amino acids in the ligand binding site with side chains capable of forming hydrogen bonds to the ligands. Aside from these three residues, the binding site is mostly hydrophobic and is thus appropriate for binding the endogenous steroid ligand, estradiol (E2) (Scheme 1). For the larger antagonistic ligands, raloxifen (RAL) and 4-hydroxytamoxifen (OHT), Asp351 in H3 is well positioned to hydrogen bond to the side chain of the ligand.

The major differences between the three conformations of the ERα LBD are the position of H12, which confer the specific activity, the lengths of H11 and H12 as well as the separation of the N-terminal of H3 and the C-terminal of H11, along with the position of the Ω-loop (*25*). In the apo conformation, H12 is extended away from the protein and is assumed to be fully solvated in the monomer. In the crystal structure used to model the apo conformation, H12 is interacting with the other monomer of an LBD dimer. This cross-monomer interaction is an artifact of the crystal structure. As pointed out by Tanenbaum et al., H11 and H12 in two neighboring monomers were synthetically linked with a disulfide bond (*20*). This constrains H12 of one monomer to interact with the LBD of the other monomer. A close inspection of the crystal structure (pdb entry 1A52) reveals that H12 is indeed very flexible because very large Debye−Waller factors are reported (*20*). When comparing one monomer from this artificial conformation of ERα LBD to known apo structures of other NRs, it becomes obvious that there is a great resemblance (*12*, *20*, *26*, *27*). Thus, we believe it serves as the best available model of an apo conformation of ERα LBD. In the agonist conformation, H12 is closed over the binding site, being held in place by what has been termed a "mouse trap" (*7*, *27*), thereby assisting in creating a co-activator binding groove between H3, H4, and H12. In the antagonist conformation, however, H12 occupies a part of the co-activator binding groove. This inhibits the binding of the co-activator protein, and consequently, dimerization and transcription activation is prevented, explaining the antagonistic activity of these ligands.

In 1964, Belleau introduced the concept of macromolecular perturbation theory (*28*), accounting for the unique conformational adaptability of enzymes when interacting with various ligands, and he extended the idea to also include receptors. Very recently, this concept of a conformational ensemble as a necessity to account for the properties of macromolecules has gained much interest in the study of protein folding and function (*29*) as well as enzyme catalysis (*30*−*33*). As the different structures became available for the various NR LBDs, it became evident that a large conformational change must accompany the biological function of this class of proteins, and the concept of a "canonical structure" of the LBD was born (*11*). This model was further developed for the ERα LBD by Moras and co-workers (*34*), who proposed a "dynamic model where H12 occupies two more or less favourable states". They termed this a "flip-flop" mechanism for the positioning of H12 (*6*), where the equilibrium between ERα conformations with the two positions of H12 (agonist or antagonist) can be perturbed by point mutations or by the presence of various other compounds such as cofactors (*34*). The two possible positions of H12 are guided by specific interactions with the remaining parts of the protein, the "mouse trap" (*7*, *11*) when H12 is resting in the agonist position and the "charge clamp" (*12*) when it resides in the co-activator binding groove as is the case for the antagonist structures. This "charge clamp" is slightly different than when acting on co-activator proteins, which are partially held tight by interaction with a residue within H12, namely, Glu542. Instead, His373 in the N-terminal of H4 interacts with Tyr537 in H12 in the antagonist structure of ERα LBD (*22*). Moras and co-workers presented a proposal for the sequence of events during the activation of ERα LBD (*23*), where ligand binding to the apo conformation precedes any conformational changes of the protein. The opposite sequence of events was recently presented by Norman et al. (*35*); in their receptor ensemble model, a rapid dynamic equilibrium between the three ERα

LBD conformations exists. They suggest that each receptor conformer can preferentially bind different ligands, meaning that ligand binding and any selectivity is determined by the conformation of the protein. No effort was presented in any of these articles to account for the binding of a co-activator protein, as to whether it precedes ligand binding and conformational changes or not. Neither was the timing of homo-dimerization included in these proposals (*23*, *35*).

The sequence of events, ligand binding, conformational change, cofactor binding, and homo-dimerization accompanying ERα LBD activation has not yet been established. Much discussion, however, is currently ongoing in the literature with respect to the allosteric control of ERα LBD. How is the information regarding the type of ligand bound in the ligand binding cavity communicated to the transcriptional machinery of ERα (*7*, *36*−*39*)? It is imperative that the specific ligand bound to the protein is somehow connected to the recruitment of cofactors and *vice versa*. However, the means of actual coupling is still poorly understood (*37*). It has become evident that amino acid residues also distant from the ligand binding cavity are involved in an allosteric network that links the functional surface of NR LBDs to the presence of a ligand in the ligand binding cavity (*36*, *37*, *39*).

Rapidly increasing scientific evidence suggests that a variety of chemicals released to the environment are xenoestrogens. Termed endocrine-disrupting compounds (EDCs) (*40*), they can interfere with hormonally regulated biological processes, as in transcription mediated by the ER (*41*−*47*). EDCs come from many different sources, such as natural products, various pesticides, pharmaceuticals, and other industrial compounds (*41*, *46*). Recent research has focused on developing analytical techniques for identifying any endocrine action of an environmental sample (*40*) or predicting eventual risks from computer studies (*48*). It has been shown that some pesticides give rise to an agonistic behavior of ER, others lead to antagonistic responses (*49*, *50*), whereas some, including DDE (a metabolite of the pesticide DDT), give rise to an entirely different response, as the induced ER conformation recognizes neither co-activators nor co-repressors related to the classical responses; rather, they adjoin different regulator peptides (*51*). This finding was interpreted as these compounds being able to induce yet another conformation of the ER LBD with different surface properties and, thereby, interfere in the transcriptional process in a different manner, further supporting the ideas of a ligand sensitive conformational equilibrium between the different conformations of the LBD (*52*) and indicating that (weak) binding of EDCs may be sufficient to disturb the position of this very delicate conformational equilibrium. Very little detailed information on how all these events are controlled at the molecular level are available, and the dynamic parts of the protein machinery are not yet fully understood.

Even though the crystal structure of ERα LBD has been known since 1997 (*19*), very little effort has been assigned to modeling the conformational changes that are so evident from a simple inspection of the different static structures. The sequence in which these events occur for ER has, to the best of our knowledge, neither been targeted through dynamic studies (e.g., NMR), nor through computer simulations. For the retinoic acid receptor (RAR), a simulation of the agonist-to-apo conformational change of the LBD has been published, suggesting that ligand dissociation is connected with minor conformational changes of H12 (*53*). From simulations of LBDs of RAR and the thyroid receptor (TR), three ligand binding/unbinding pathways have been observed (*53*−*56*). Very recently, a new study of the RAR LBD using random expulsion MD identified a fourth possible escape pathway between H12 and the N-terminal of H3 in an agonist conformation of the protein (*57*). These five studies revealed that the identified pathway depends on the specific setup of the simulation, on the NR, and on whether mutations are present in the starting structure of the protein as well as the structure of the ligand. Nonetheless, some overlap between the proposed pathways was found. It is obvious that the sequence of events and the actual pathways may not be directly transferable between different NRs. Importantly, none of these simulations included the co-activator protein, which may obstruct some of the observed escape routes. However, the results are very promising in showing how MD simulations can help in disentangling reaction sequences and revealing the dynamics of larger conformational changes of proteins. In recent years, MD simulation has proved to be a valuable tool for studying the dynamic behavior of macromolecular systems (*58*−*61*), and the method is complementary to static X-ray diffraction methods. Especially, for elucidation of the dynamic pathways of biological transport mechanisms (*62*−*66*) and conformational changes (*29*, *67*, *68*), MD techniques have recently been very successful in providing additional knowledge of such complicated biochemical reactions.

In this article, we present the results of a total of 158 ns unrestrained all-atom MD simulations of the hERα LBD. The focus will first be on describing the binding of the endogenous ligand, E2, with respect to the preferred charge and tautomer of His524 in the agonist conformation of hERα LBD and the influence of the co-activator protein on this binding. To the best of our knowledge, this is the first time that a model of the co-activator protein has been included in simulations of a NR LBD. We model the co-activator protein with a small peptide with the conserved LXXLL motif, NAL***LRYLL***D (copep). Experimental studies have shown that this motif is "necessary and sufficient to mediate the binding of these proteins" and that peptides with this motif "contained within as few as eight amino acids is sufficient to bind to transcriptionally active NRs" (*13*); thus, this 9-amino acid model peptide should represent a realistic model. Then, the conformational changes of the LBD will be examined from several long time MD simulations of the apo and the agonist conformations with and without the ligand and copep present. Because H12 is not localized at the dimerization interface, we expect that dimerization will not be greatly influenced by H12 positioning. Therefore, we have chosen to model the monomer of hERα LBD instead of the dimer. This is similar to all other simulations on NR LBDs in the literature (*53*−*57*). The putative switching, or flip−flop mechanism (*6*, *23*, *34*, *51*, *52*) of H12 between either covering the ligand binding pocket, as caught in the "mouse trap", or resting in the co-regulator binding groove is also examined by MD simulations of the antagonist conformation. From the simulations, we propose a likely sequence of events, ligand binding, copep binding, and conformational changes of H12, required for the formation of a transcriptional active complex, and we will discuss the

proposed agonist-to-antagonist conformational changes. We present a likely allosteric mechanism for linking the two focal points for activation of the ERα LBD, namely, ligand binding and positioning of H12, and we also present results that shed light on the pivotal role of His524 in ligand binding and activation of hERα LBD.

MATERIALS AND METHODS

The apo and agonist conformations of hERα LBD, both with co-crystallized E2, and the antagonist conformation with co-crystallized OHT were chosen as starting protein structures. Atomic coordinates were taken from the Protein Data Bank (*69*), entries 1A52 as a model for the apo conformation (*20*), 1GWR for the agonist conformation (*21*), and 3ERT for the antagonist conformation (*22*). The proteins contain 238 (apo), 243 (agonist), and 246 (antagonist) amino acid residues in the modeled monomer, all starting from Leu306. The co-crystallized copep, with sequence NAL***LRYLL***D from the agonist structure pdb entry 1GWR, was used in simulations of apo as well as agonist conformations with a copep present. The residues are numbered 1−9. The termini were modeled as charged. No efforts were taken to include the approximately 45 missing amino acid residues of the F-domain in the C-termini of the structures because their function and structure are unknown (*6*). It is speculated that the flexibility of H12 cannot be hampered much by the inclusion of this small domain because only the flexibility of a loop is required. Most importantly, the presence of more than 60 NR crystal structures, including either the DNA binding domain or the LBD as well as experimental studies on the LBD alone, indicate that the different domains are not dependent upon each other for activity.

Coordinates for the backbone atoms in two loops, between H2 and H3 and between H8 and H9, were missing in the agonist conformation. These were modeled by including coordinates for residues 331−339 and 461−465 from pdb entry 1A52 into the agonist protein structure. These residues later underwent special treatment during the minimization of the system. Several residues in the three conformations were solved to multiple positions in the X-ray structure, and their treatment is included in the Supporting Information. Coordinates for missing amino acid side chains and hydrogen atoms were reconstructed with the psfgen structure builder module of NAMD (*70*) and by using the CHARMM27 force field (*71*). The system was solvated in a pre-equilibrated water box using the solvate plug-in in VMD and extending 10 Å beyond the protein. The TIP3P water model was used (*72*). This solvation resulted in systems with overall sizes of approximately 80 × 100 × 60 Å^3 (apo), 80 × 80 × 60 Å^3 (agonist), and 80 × 80 × 80 Å^3 (antagonist) and contained approximately 40,000 (apo and antagonist) and 30,000 (agonist) atoms. All crystal water molecules were kept in the simulations.

Amino Acid Protonation States. There are 13 histidine residues in the hERα LBD. One of these, His524, is positioned in the binding pocket and hydrogen bonds the ligand; it is, thus, important for appropriate ligand binding. In all X-ray agonist structures of the hERα LBD, His524-(Nδ) is pointing toward E2(O17) (see Scheme 2 for the numbering of atoms), indicating a preferred binding mode. However, because hydrogen atom positions cannot normally

Scheme 2: Coordination of E2 in the Ligand Binding Cavity[a]

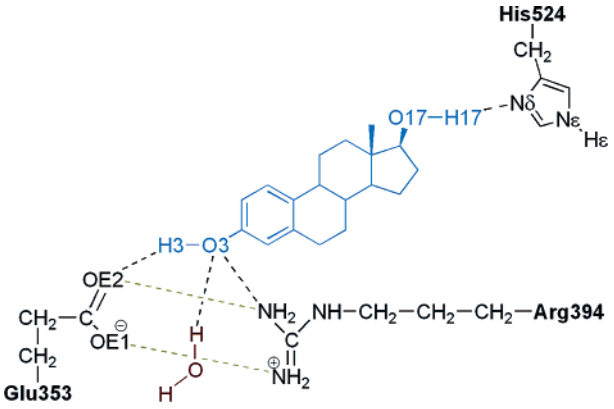

[a] Important atoms in E2 (blue) and the surrounding residues are labeled. His524 is drawn as the ϵ-tautomer. In the δ-tautomer, the proton would be located on Nδ (denoted Hδ), whereas in the imidazolium ion of charged His524, both hydrogen atoms as well as a delocalized positive charge are found. A crystallized water molecule (brown) also interacts with E2.

be determined by X-ray crystallography, there is no direct evidence of the charge and tautomer state of His524. It is, therefore, not a straight forward decision as to whether His524 or the ligand acts as the hydrogen bond donor or acceptor because both can act as such depending on the charge and tautomer of His524 and the orientation of the E2 hydroxyl group. To study this issue, simulations were set up with both of the neutral tautomers of the imidazole ring in His524 as well as the charged form, by incorporating an imidazolium ion for each of the models studied. Other histidine residues were modeled according to their local environment (see Supporting Information for details), whereas all Arg, Lys, Asp, and Glu residues were modeled as charged and all tyrosines as neutral. By changing the charge of His356 in H4, which is distant from the binding site and is surface exposed, at the same time as that of His524, the system is kept neutral in all setups.

Modeling Estradiol. Force field parameters to model E2 were extracted from the CHARMM27 force field (*71*) and supplemented by parameters from a very recent simulation including cholesterol for the steroid skeleton (*73*) as well as Accelrys-CHARMm parameters as included in Quanta 2000 (*74*). Partial charges for E2 were calculated with VCharge (*75*) by equalization of electronegativity. This method has recently been shown to give charges very similar to those in the CHARMM force field (*75*). Partial charges and added parameters for force constants and Van der Waals terms are tabulated in the Supporting Information. The initial structure of E2 was extracted from the pdb file of the agonist structure (*21*) and used in all of the agonist and antagonist simulations. Because E2 is not naturally found in the antagonist conformation, it was manually positioned with the steroid A-ring on top of the phenol ring of the co-crystallized OHT positioning the E2(O3)-hydroxyl group to hydrogen bond with Glu353 and Arg394. In the apo simulations, the co-crystallized E2 from pdb entry 1A52 (*20*) was used.

Minimization. The solvated systems were minimized with NAMD (*70*) using the conjugate gradient algorithm twice for 2500 minimization iterations to remove the steric strain introduced when adding hydrogen atoms and missing side

Table 1: Ten hERα LBD Models with Information about the Initial Conformation of the Protein, the Presence of E2, and a Co-Activator Peptide[a]

	initial conformation	ligand	co-activator peptide	to study
1	agonist	E2	NAL***LRYLL***D	E2 binding in biologically relevant form; evaluate charge and tautomer of His524
2	agonist	E2	none	the influence on E2 binding in the absence of copep
3	agonist	None	none	the stability of agonist conformation of the protein without E2
4	agonist	None	NAL***LRYLL***D	the stability of agonist conformation without E2 but in the presence of copep
5	antagonist	E2	none	antagonist conformation with E2
6[b]	antagonist	E2	none	antagonist conformation with E2 at higher temperature
7[c]	apo	E2	none	stability of the apo conformation with E2 bound
8	apo	E2	NAL***LRYLL***D	the influence of copep on apo conformation with E2 bound
9	apo	none	none	the stability of the apo conformation, only protein
10[d]	apo	none	NAL***LRYLL***D	the stability of the apo conformation, including copep

[a] The purpose of studying each model is listed. [b] Model **6** is simulated at 400 K. [c] Model **7E** is simulated for 12 ns. [d] Model **10P** is simulated for 6 ns.

chain atoms. During the initial 2500 minimization steps, only hydrogens were allowed to move while all heteroatoms were kept fixed. In the second set of minimization, heteroatoms were restrained in a harmonic potential with a force constant of 0.5 kcal/(mol·Å^2). All atoms in the two loops that were originally missing coordinates in the agonist structure were allowed to move freely during both sets of minimizations.

Molecular Dynamics Simulations. All simulations were performed using the CHARMM27 force field (*71*) with the added parameters for E2 by using the MD program NAMD 2.5 (*70*) on 32 processors. The MD simulations were performed in the NPT ensemble with periodic boundary conditions. For full employment of electrostatics, the particle mesh Ewald method (*76*) was employed, whereas Van der Waals interactions were accounted for to a cutoff distance of 12 Å and gradually dampened by use of a switching function from 10 Å. Langevin dynamics with a damping constant of 0.1 ps^{-1} was included to achieve constant temperature, whereas the atmospheric pressure was realized with the Langevin piston method as implemented in NAMD (*77*). A total of 10 different setups, models **1**−**10**, of the system were investigated (see Table 1 for details). Three simulations were run for each model to account for the three possible forms of His524, labeled, for example, for model **1** as **1D**, **1E**, and **1P**, for the δ-tautomer, ϵ-tautomer, and positively charged forms of His524, respectively, resulting in a total of 30 simulations. All simulations were carried out for at least 5 ns using a 1 fs time step, and snapshots for analysis were saved every 500 fs.

Data Analysis. Analysis of the computed trajectories was performed with VMD 1.8.3 (*78*) and the included Tcl-scripting facility. All molecular figures were drawn in VMD. The root-mean-square-deviation (RMSD) of protein Cα atoms in each simulation was calculated with respect to the initial minimized structure. To measure the length of H11, backbone N···O distances from residues n to $(n + 4)$ are measured. If this distance is less than 3.5 Å, then the $(n + 4)$ residue is supposed to be included in H11. This is slightly longer than the normal hydrogen bond distance of approximately 3 Å (*79*) and is included to allow for breathing in the helix.

RESULTS AND DISCUSSION

We first set up systems to study the hERα LBD in the agonist conformation with bound E2. Models **1** and **2** investigate the stability of this conformation and the influence of the copep on binding of the endogenous ligand. Model **1** represents the functional biological form of the receptor; it can, therefore, be used to imply whether the applied protocol for modeling is reliable. Model **2** examines the binding of E2 in the absence of copep, whereas models **3** and **4** were included to evaluate the stability of un-liganded hERα LBD in the agonist conformation. The influence of the bound copep is studied in models **1** to **4** for the agonist conformation where simulations with copep are done in the presence or absence of E2, respectively. Furthermore, we set up simulations that were likely to result in conformational changes; the intention being to construct some of the protein−ligand complexes proposed to be involved in the mechanism of the structural transition from the transcriptionally inactive apo form to the active agonist form with ligand and copep bound (*23*). Models **5**−**10** are constructed to evaluate exactly such conformational changes. The two first sets, models **5** and **6**, investigate the dynamics of the antagonist form when it is bound to E2 at different temperatures. With this setup, one may then expect to observe a conformational change from the antagonist form to either the apo or agonist conformation. Such a mechanism has been proposed by Moras and co-workers (*11*, *23*) and Shiau et al. (*52*) and has been further interpreted as a "switching mechanism of H12 between capping the ligand binding cavity and the co-regulator

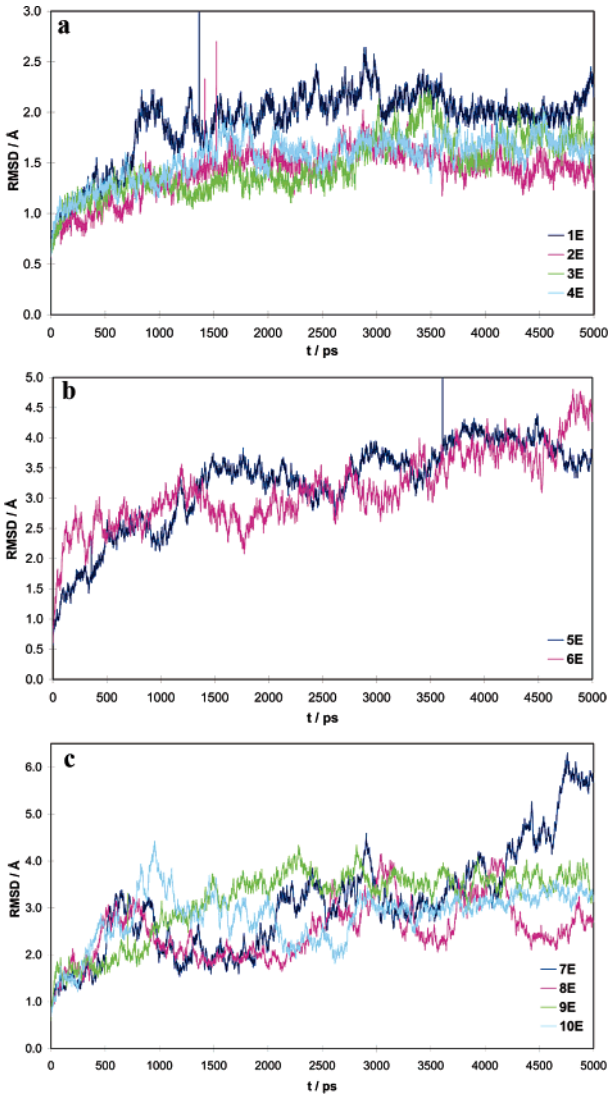

FIGURE 2: RMSD of Cα atoms of the hERα LBD throughout simulations for (a) agonist models **1**−**4**, (b) antagonist models **5**−**6**, and (c) apo models **7**−**10**, all with His524 modeled as the ϵ-tautomer. Data for the δ-tautomer and charged His524 can be found in the Supporting Information.

binding groove" (*51*) very similar to the flip−flop mechanism, which states that the two binding sites of H12 have very similar binding energies (*34*). Because model **5** at 310 K did not reveal much instability in the protein (*vide infra*) a similar simulation, model **6**, at an elevated temperature was undertaken in order to force some conformational changes to occur. The next four models, **7**−**10**, are simulations of the apo conformation and are included in the study to test the hypothesis that the biologically active form of hERα LBD is produced from the apo form by the binding of E2 and/or copep followed by conformational changes (*23*) or the *vice-versa* (*35*). In models **8** and **10**, the influence of a copep is further studied for the apo conformation of the protein. Models **3**, **4**, **9**, and **10** were included to observe the stability of the ligand binding site of hERα LBD and to evaluate whether the binding cavity collapses without a bound ligand, similar to what has been described for the retinoid-X receptor α (*24*). It was recently shown that some EDCs recognize another conformation of hERα LBD (*51*); thus, it was of great interest to us to test if such (quasi) stable conformations could be identified from the MD simulations.

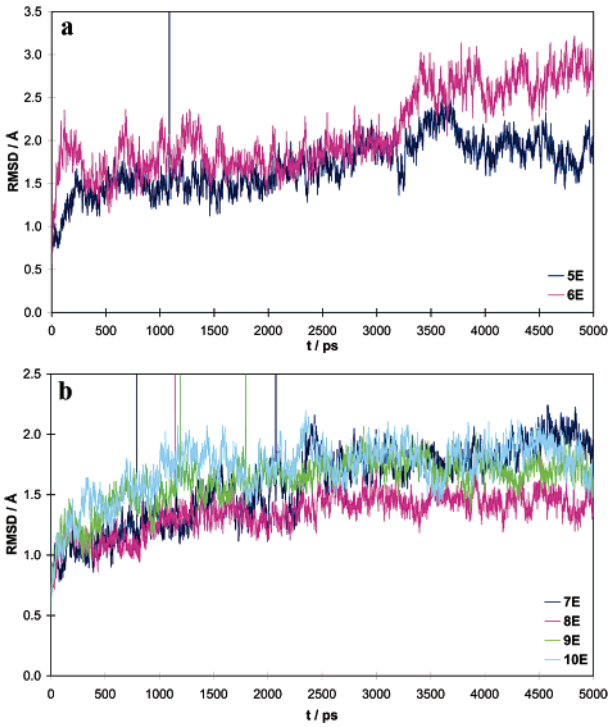

FIGURE 3: RMSD for hERα Cα atoms in the LBD core during simulations for (a) antagonist models **5**−**6** and (b) apo models **7**−**10**. All Figures have His524 in the ϵ-tautomer. Plots with the two other forms of His524 are found in the Supporting Information.

Conformational Stability of Simulations. For all simulations, the calculated RMSD for all Cα atoms reaches a stable value after approximately 1 ns. The agonist models **1**−**4** reach a value of ∼1.8−2.0 Å, the antagonist models are more dynamic and have RMSD values between 2 and 4 Å, and the apo models show even more movement, leveling out at 2−5 Å (Figure 2). Initially, this may indicate unstable simulations of the antagonist and apo models, but because these calculations were set up to investigate conformational changes of, especially, H12, it is not surprising to get such rather high rmsds. Therefore, another set of RMSDs curves were calculated, including only Cα atoms in residues 306−527, these curves are displayed in Figure 3 for antagonist and apo models. In this way, the last coil of H11, the loop H11−H12, and H12 itself are not included in the RMSD calculation, and thus, only the stability of the LBD core of hERα is calculated. Using this scheme, the simulations of models **5** and **7**−**10** gave RMSD values of approximately 1.8−2.0 Å, similar to what is found for the whole protein in the agonist conformation. The RMSD value for model **6,** which was run at a higher temperature of 400 K, is logically somewhat higher and levels out at 2.5−3.0 Å.

These results show that the dynamics are mostly associated with the H11−H12 region for the simulations of antagonist and apo models. The RMSD of the agonist model **1**−**4** did not change when excluding the C-terminal residues, showing that all agonist simulations are carried out on stable structures, also in the absence of ligand E2 and/or the copep. It can, thus, be concluded that equilibrated systems are obtained after approximately 1 ns in all models.

Conserved Hydrogen Bonds. X-ray structures of the hERα LBD indicate the presence of hydrogen bonds between E2(O3) (see Scheme 2 for the numbering of atoms) and the side chains of two residues, namely, Glu353 and Arg394, in

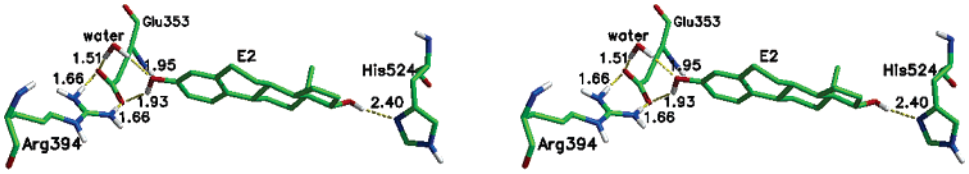

FIGURE 4: Stereoview of E2 in the binding site of hERα LBD (snapshot of model **1E** at 1.5 ns) with Glu353, Arg394, and His524. A structural water molecule is present that further links E2 and Glu353. Average distances between interacting heteroatoms are listed in Ångstrøms.

the binding site. In the X-ray structures, a water molecule is similarly responsible for yet another stabilizing hydrogen bond between E2 and the protein. During the extent of all of the present simulations, a hydrogen bond can be identified to one of the carboxylic oxygen atoms of Glu353, most often to Glu353(OE2), which is positioned closest to E2 in the agonist and apo X-ray structures. A rotation of the side chain is possible and results in hydrogen bonding the Glu353(OE1) instead. A direct hydrogen bond to Arg394, however, is not present in the simulations, evidenced from average distances between E2(O3) and the two terminal nitrogen atoms of Arg394 of more than 4.2 Å. Rather, the Arg394 side chain moves slightly to form two ionic hydrogen bonds to Glu353. In NRs with a keto functionality on the A-ring of the steroid ligand, Glu353 is replaced by a glutamine residue, thereby favoring hydrogen bonds from both residues to the ligand, whereas the hERα LBD system seems to be stabilized by the interactions of the formal charges at residues Glu353 and Arg394. In Figure 4, the resulting hydrogen bond network between E2(O3), Glu353, Arg394, His524, and a binding site water molecule is displayed.

It was recently shown by Moras and co-workers (*39*), that two conserved hydrogen bonds are found in all class I NRs (homo-dimers). They proposed that these hydrogen bonds are present to facilitate communication between the co-activator binding site (Glu323 in Helix1) and the dimerization interface (Arg503 in helix10). The communication pathway passes through helix8 (Lys449 and Glu444). These two hydrogen bonds are conserved in all of the simulations (data not shown), further revealing that the monomer modeled is indeed in accordance with the monomers of the crystallized dimers.

Agonist Conformation. The binding of E2 in the biologically active transcription complex of hERα LBD with a bound copep is studied in model **1**. Three simulations were carried out to elucidate the likely protonation state of His524, models **1D**, **1E**, and **1P**. On the basis of X-ray structures (*19*, *21*, *22*, *34*, *80*, *81*), it is believed that there is a hydrogen bond between His524(Nδ) and E2(O17). However, with X-ray diffraction techniques, it is normally not possible to refine the hydrogen atom positions in protein crystals; therefore, all three possibilities are explored in this study. Recently, we have shown that MD simulation is a suitable tool for assigning the protonation state of important residues in protein−ligand complexes (*82*, *83*). Similar methodology is applied here, focusing on identifying the charge and tautomer of His524 that gives rise to the most stable hydrogen-bonding pattern.

In Figure 5, plots of the distance between His524(Nδ) and E2(O17) and the corresponding hydrogen bond angle are displayed for the three simulations of model **1**. It is apparent that only model **1E**, with the ϵ-tautomer of His524, has the hydrogen bond between E2(O17) and His524(Nδ) conserved

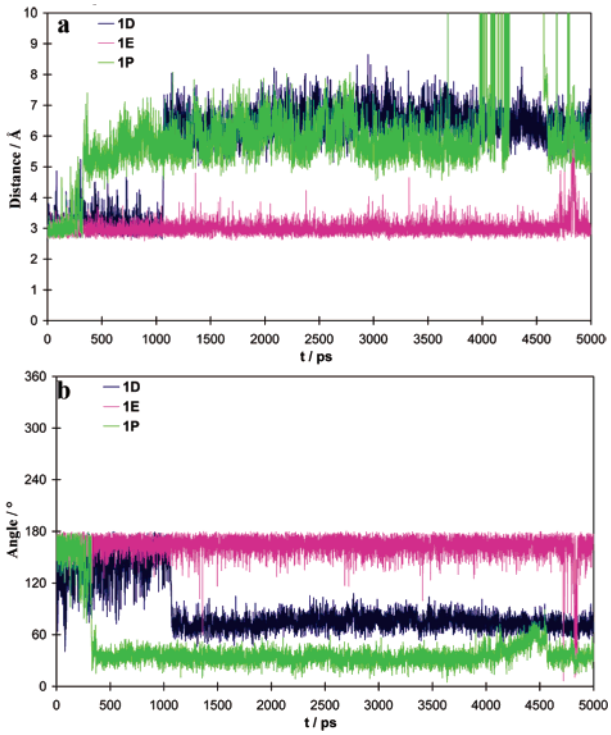

FIGURE 5: (a) Hydrogen bond distance E2(O17)···His524(Nδ) in models **1D**, **1E**, and **1P** and (b) the corresponding E2(O17)···H···His524-(Nδ) angles. For **1D**, H = Hδ, and for **1E** and **1P**, H = H17.

throughout the simulation. This means that E2 is the hydrogen bond donor, and His524 is the hydrogen bond acceptor. Also, the angle for the hydrogen bond is stable, with an average of 163 ± 12°. Neither the δ-tautomer nor a charged His524 are able to retain the conserved hydrogen bond throughout the simulation. These two forms of His524 rotate after approximately 1 ns; therefore, the imidazole ring system becomes almost perpendicular to the E2 D-ring with E2(O17)···His524(Nδ) and E2(O17)···His524(Nϵ) distances of 6−8 Å being too long for a hydrogen bond to form.

From the X-ray experiments, it is suggested that His524 is placed in a rather shallow potential on the energy surface because it occupies only one position and has normal Debye−Waller factors. The average dihedral angles for the side chain of this amino acid is experimentally found to be a gauche conformation for χ_1 (C-Cα-Cβ-Cγ), measuring 45−60°, and a −gauche conformation for χ_2 (Cα-Cβ-Cγ-Nδ) between −70° and −90°. The distribution in the two dihedral angles as a function of time is depicted in Figure 6 for the MD simulations of model **1**. Again, it is obvious from the curves that only an ϵ-tautomer of His524 gives a dihedral angle distribution that is in accordance with the experimentally observed numbers; hence, the simulations of model **1** support that His524 is neutral and found as the ϵ-tautomer and functions as a hydrogen bond acceptor, whereas the ligand is the hydrogen bond donor.

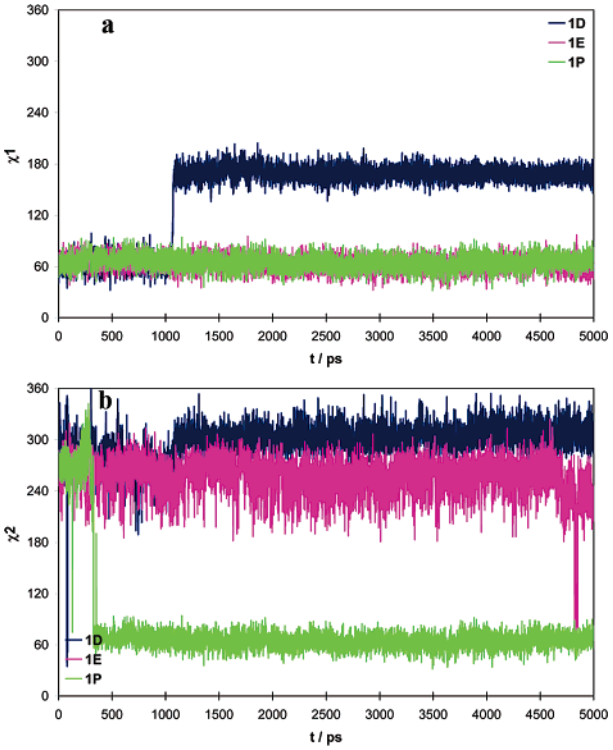

FIGURE 6: Variation in the dihedral angles of the side chain of His524 in simulations **1D** (blue), **1E** (magenta), and **1P** (green); (a) χ_1 and (b) χ_2.

During the three simulations of model **1**, H12, which has been proposed to function as a lid of the ligand binding cavity, is held in the agonist position by the "mouse trap" mechanism. H12 is positioned in the groove between H3, H4, and H11 and is mainly held tight by hydrophobic interactions. The binding of the copep is also stable in all model **1** simulations. The copep is positioned in a shallow hydrophobic groove between H3, H4, and H12 and held in place by the so-called "charge clamp" made from Lys362 in H3 and Glu542 in H12 (*3*, *19*). The former is coordinated through the three hydrogen atoms at Lys362(NZ), forming hydrogen bonds with Leu7(O), Tyr6(O) and Asp9(OD2) of the copep in a nice tetrahedral manner, whereas Glu542 interacts with Ala2(NH) and Leu3(NH). The LXXLL motif of the copep is made up by Leu4 to Leu8. These findings suggests that on this time-scale, the finer details in the ligand binding cavity, as expressed in the three setups of model **1**, do not influence surface properties as judged by the binding of H12 and copep.

On the basis of a triple Cys → Ser mutation study of ERα LBD, Moras et al. (*34*) proposed that the biologically active agonist conformation is partly stabilized by the presence of a conserved hydrogen-bonding network zipping H3 and H11 together, originating at the His524 side chain in the ligand binding pocket and terminating at Lys531 in the C-terminal of H11 and Glu339 in the N-terminal of H3 via Glu419. We have analyzed the presence of such a network with respect to the selection of the charge and tautomer for His524. The computed frequencies for the formation of the hydrogen bonds involved in the zipper are listed in the Supporting Information. In model **1E**, this hydrogen-bonding network is indeed present throughout the simulation (Figure 7), whereas it is formed much less frequently in **1D** and **1P**. In conclusion, model **1E** must be a reliable setup for the biological active structure of hERα LBD because all experimental data available are nicely reproduced in this model, and we conclude that the present MD simulation protocol represents an appropriate method for studying this system.

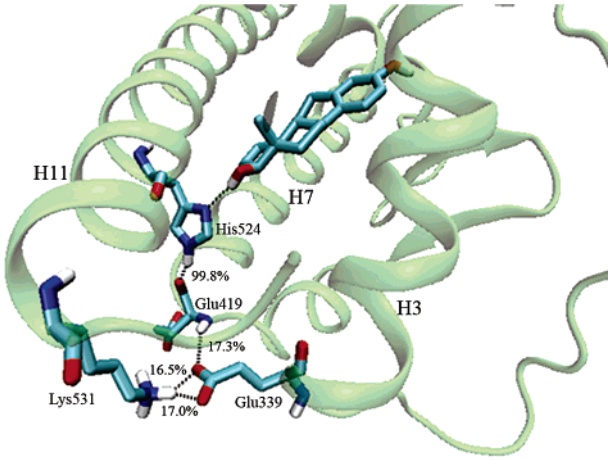

FIGURE 7: Snapshot of model **1E** at 1.5 ns showing the binding of E2, along with the residues in the hydrogen bond zipper. Numbers are included for the presence of each hydrogen bond during the trajectory.

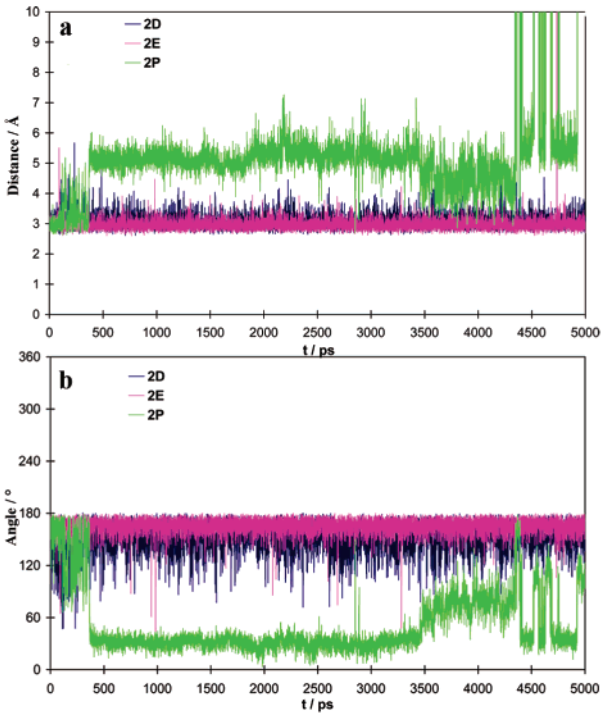

FIGURE 8: Time dependence of (a) hydrogen bond distance E2(O17)···His524(Nδ) in models **2D**, **2E**, and **2P**; (b) the corresponding E2(O17)···H···His524(Nδ) angle. For **2D**, H = Hδ, and for **2E** and **2P**, H = H17.

We next studied the agonist complex, where E2 is bound, and H12 is capping the ligand binding site but without the copep (model **2**). These simulations will reveal the influence of a copep on the stability and dynamic properties of the system upon comparison with model **1**. Focusing first on the interaction of E2(O17) with His524, the three simulations, **2D**, **2E**, and **2P**, reveal that the hydrogen bond E2(O17)···His524(Nδ) can be maintained for both of the neutral tautomers of His524. The curves are shown in Figure 8 for the E2(O17)···His524(Nδ) distance and the corresponding bond angle.

Without the copep bound to the complex, more flexibility in the choice of the tautomer of the neutral His524 seems to be possible because both models **2D** and **2E** show a conserved hydrogen bond from E2(O17) to His524(Nδ) throughout the simulation. In model **2E**, the distance of E2(O17)···His524(Nδ) is 2.96 ± 0.17 Å, and the angle of E2(O17)···H···His524(Nδ) is 165.1° ± 8.9°. The same geometric properties for model **2D** are 3.08 ± 0.23 Å and 153.4° ± 16.5°, respectively. Again, a charged His524 is not suitable for conserving this hydrogen bond because the residue rotates. In model **2D**, a rotation around the E2(O17) hydroxyl bond has taken place; therefore, E2 is now the hydrogen bond acceptor, and His(Nδ) is the hydrogen bond donor. An additional long hydrogen bond, 3.69 ± 0.44 Å, between E2(O17) and Gly521(O) was found to further stabilize this model. This is similar to what has been proposed for the binding of E2 in ERβ (*52*). With respect to the hydrogen-bonding network originating at His524, it is conserved in model **2E** with the number of hydrogen bonds present very similar or slightly larger than that found for **1E**. In model **2D**, however, only the distance from His524(Nϵ) to Glu419(O) remains below the limiting 4.0 Å, with an average of 3.87 ± 0.75 Å. This must be a very unfavorable situation because of the lack of an intermediate hydrogen atom, and we expect model **2D** to be unlikely on this basis. The rest of the hydrogen bonds are lost very early in the simulation of model **2D**. However, no further conformational consequence of this un-zipping of H3 and H11 can be detected because the length of H11 is conserved and terminates at Asn532 in all setups. (The computed frequencies for the α-helical length of H11 are listed in the Supporting Information.) This suggests that once H12 is placed in the "mouse trap" position, it is firmly bound, and even the un-zipping of H3 and H11 does not influence the binding of H12 on this time scale.

The simulated trajectories of models **3** and **4**, both without E2, reveal that the protein is stable on a nanosecond time scale in the agonist fold with neither copep nor the ligand bound (models **3**) as well as in a setup including copep but without the ligand (models **4**). In model **4D**, the length of H11 is slightly shortened, indicating that the presence of the copep can induce some changes in the finer details of the conformation. This effect is not seen for other forms of His524, nor in any setup in model **3**. Because the ligand binding cavity is empty in models **3** and **4**, His524 is not anchored to the ligand. In these simulations, a rotation of His524 is observed changing from −gauche for χ_2, which is found in agonistic protein crystal structures. Instead, both χ_1 and χ_2 are in the +gauche conformation. After ∼1.5 ns of simulation in model **4D**, both χ_1 and χ_2 dihedral angles shifts to the −gauche conformation, still unlike the experimentally observed conformations. This is additionally revealed in the computed number of possible interactions between His524 and Glu419(O), where it is evident that His524 is flexible in the absence of copep (model **3**). The inclusion of a copep in the simulations of models **4E** and **4P** results in a completely locked orientation of His524. Accompanying this freezing out of any rotation of His524 is the observation that the hydrogen-bonding network is reestablished, zipping H3 and H11 together only in model **4E**, showing how the presence of a copep is communicated to the ligand binding cavity through the conservation of this hydrogen-bonding network and arresting His524 in an orientation set up for the interaction with E2 once it is present in the ligand binding cavity.

Antagonist Conformation. In models **5** and **6**, we examine the dynamical behavior of a mismatched complex between an antagonist conformation of the protein, with H12 resting in the co-activator binding groove, and an agonist ligand, E2, in the ligand binding cavity. According to the flip−flop mechanism, this situation should lead to a rearranged structure. Therefore, by running MD simulations on this unfavorable complex, the idea was to stimulate the conformational changes to proceed. As for the agonist models discussed above, the first structural feature to look for is the presence of a hydrogen bond from E2(O17) to His524. The hydrogen bond was not found for extended periods of time in any of the three examined His524 forms of models **5** and **6** during the 5 ns simulations. Another possibility would be a hydrogen bond to His524(Nϵ), but further analysis revealed this distance to be constantly larger than 5 Å for all models, thus precluding this hydrogen bond from forming.

In antagonist protein structures (*22*, *34*, *84*, *85*), His524 is rotated compared to the agonist structure, which explains the lack of formation of this hydrogen bond. We speculate that as a consequence of the rotation of His524, an unleashing of the hydrogen bond network zipping H3 and H11 together is taking place. Indeed, the simulations reveal that the network is not starting to form in any of the setups, and Glu339 and Lys531 are positioned too far away from each other to interact. This set of simulations, therefore, indicates that a direct equilibrium between the agonist and antagonist conformations may not be so likely. The very dynamic appearance of the binding site is not due to a simple continuous rotation of the His524 side chain because both χ_1 and χ_2 are alternatingly stable in +gauche, −gauche, or anti conformations. The dynamic behavior is also due to movements of the backbone of H11 and the ligand. To identify the most dynamical parts of the ERα LBD in the antagonist conformation, simulations at 400 K, where the protein is more dynamic, model **6**, were undertaken. Specifically, in model **6P**, it is noted that H12 is slightly released from the co-activator binding groove. At the same time, the small kink between H10 and H11 becomes more pronounced, and the two helices become almost perpendicular to one another. As a consequence, His524, which is located in the N-terminal of H11 near the kink, becomes surface exposed. These features will be further studied for mechanistic relevance.

Apo Conformation. We next set up models to study the dynamic behavior of the apo conformation of hERα LBD. The influence of the binding of E2 and copep is studied systematically in the four models, **7**−**10**, in order to obtain more information about the sequence for the binding of E2, copep, and the conformational changes observed in the LBD of hERα. The binary apo complex with E2 bound, model **7**, reveal that the dynamic behavior of H12 is dependent on the chosen form of His524. A new stable conformation is found in model **7D**, which is stable for the last 3 ns of the dynamics. In this alternative structure, the hydrogen bond between His524(Nδ) and E2(O17) reforms after approximately 2.0 ns. It was present in the very beginning of the

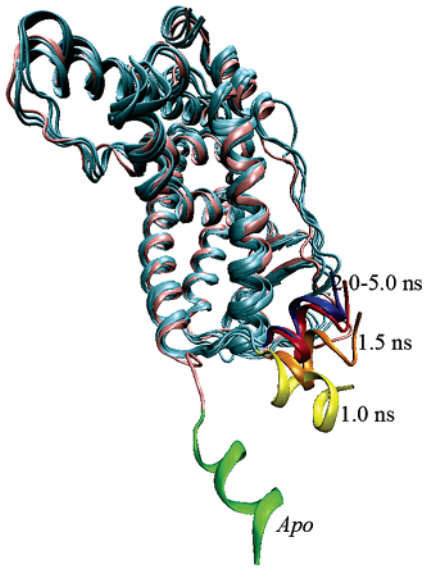

FIGURE 9: Overlay of snapshots of the conformational dynamics of model **7D**. The X-ray structure (1A52) is shown in pink with H12 in green. For the snapshots, the core of the protein is depicted in cyan, whereas H12 is yellow after 1 ns, orange after 1.5 ns, red after 2.0 ns, and blue after 5.0 ns.

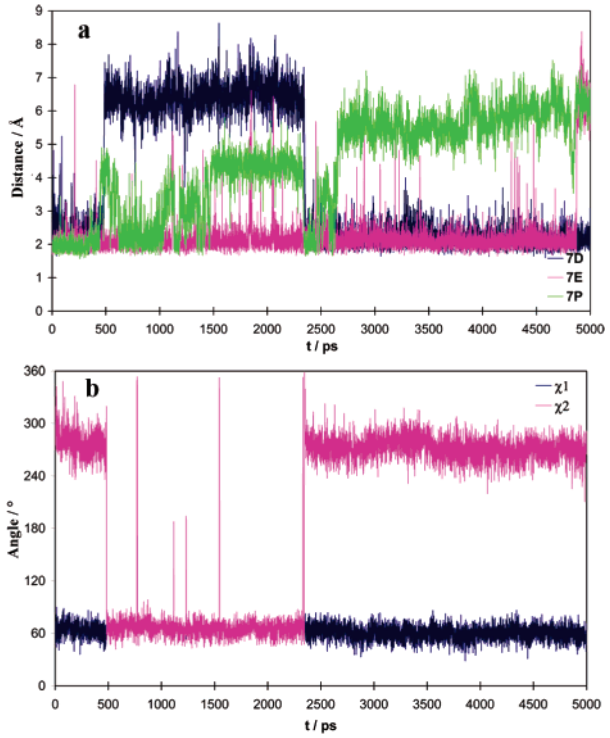

FIGURE 10: Time dependence of (a) the distance between E2(O17) and His524(Nδ) in 7 and (b) χ_1 and χ_2 in model **7D**.

simulation, but when H12 started to move after approximately 0.5 ns, the hydrogen bond broke and did not reform before the stable alternative position of H12 was reestablished (Figure 9).

Figure 10a shows the distance between E2(O17) and His524(Nδ) as a function of simulation time for model **7**. By following the dihedral angles of His524 in model **7D**, it is found that the hydrogen bond breaks because of a rotation of χ_2 from a −gauche conformation to a +gauche conformation, which changes back to −gauche as the hydrogen bond reforms (Figure 10b). Because of the lack of a hydrogen atom on His524(Nϵ), the hydrogen bond network from His524 to Glu339 cannot be fully formed throughout the **7D** simulation, but there are conserved hydrogen bonds between Lys531(NZ) and both carboxyl oxygens on Glu339, serving to keep H3 and H11 tied together. In accordance with this, it is found that H11 is not unwinding in this new alternative conformation. The binding of H12 to the core of the hERα LBD in the alternative conformation is firm on the basis of the long stability of the conformation and on computed RMSD values between snapshots taken between 2 and 5 ns of ~1.2 Å.

In model **7E**, H12 is solvent exposed during the first nanoseconds of the simulations. After 5.0 ns, snapshots indicate that H12 may be moving toward the "charge clamp" position in the co-activator binding site. Because of the possibility of a conformational change toward the antagonist conformation, the **7E** simulation was continued to 12 ns. However, instead of approaching the antagonist conformation further, the orientation of H12 once again shifted. The N-terminal of H12 is kept relatively at the same point in space, while the C-terminal moves. This leads to a position after 7.5−8.0 ns, which resembles the agonist structure. The E2(O17)···His524(Nδ) hydrogen bond is disrupted after around 4.8 ns of dynamics but is reformed for brief periods later in the simulation (6.8−7.4 and 11−12 ns). After approximately 9 ns, the otherwise conserved hydrogen bond to Glu353 disappears, and H12 is again fully flexible.

The dynamic consequences of modeling His524 as charged in the apo conformation, model **7P**, leads to a situation, where H12 is not able to bind to the core of hERα LBD. It is persistently found in a conformation mostly resembling the apo form as solvent exposed. It moves in a seemingly random way, similar to a dog wagging its tail. The effects on the dynamic properties of the binary apo ERα complexed with E2 upon the binding of a copep are studied in model **8**. A stable conformation of hERα cannot be identified from the trajectories for any of the three His524 forms. All give rise to a random dynamic behavior, similar to that in model **7P**. This observation suggests that the conformational change toward the active complex requires that copep and E2 cannot both bind to the apo conformation of hERα prior to changing the conformation of the protein.

Finally, the dynamics of apo hERα LBD is studied in the absence of a ligand in the binding site (models **9** and **10**). Interestingly, these simulations reveal a semi-stable conformation as well as new mechanistic aspects of the activation mechanism. In model **9E**, a new conformation is found for about 1 ns during the simulation, and this conformation is then reformed during the final nanosecond. Further studies are in progress for this model. In model **10P**, with a copep bound to the apo conformation of hERα LBD, dramatic changes in the behavior of the binary complex is observed. H12 is very dynamic and travels toward the agonist position. After 6.0 ns, H12 is positioned in the extension of its agonistic position in the "mouse trap". Snapshots of this conformational change are included in Figure 12a, and the end-point of **10P** is overlaid upon the agonist structure in Figure 12b.

It is furthermore seen that His524 becomes surface exposed during the dynamics of H12 because of a kink between H10 and H11, hindering the formation of the hydrogen bond zipper. This can be observed by counting

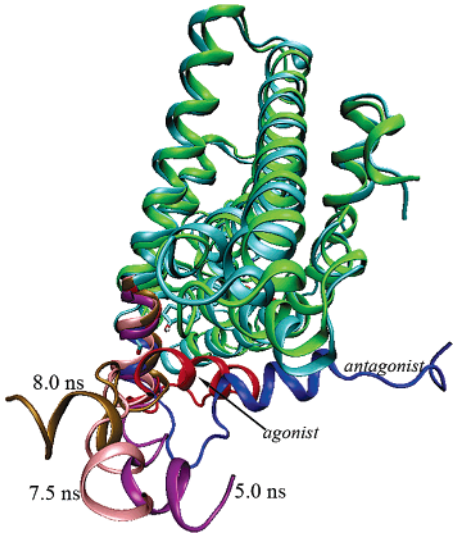

FIGURE 11: Snapshots from the simulation of model **7E** at 5.0 ns (H11−H12 in purple), 7.5 ns (H11−H12 in pink), and 8.0 ns (residues 306−520 in cyan and H11−H12 in brown). Also included are agonist (H11−H12 in red) and antagonist (residues 306−520 in green with H11−H12 in blue) X-ray structures with pdb entries 1GWR (*21*) and 3ERT (*22*), respectively.

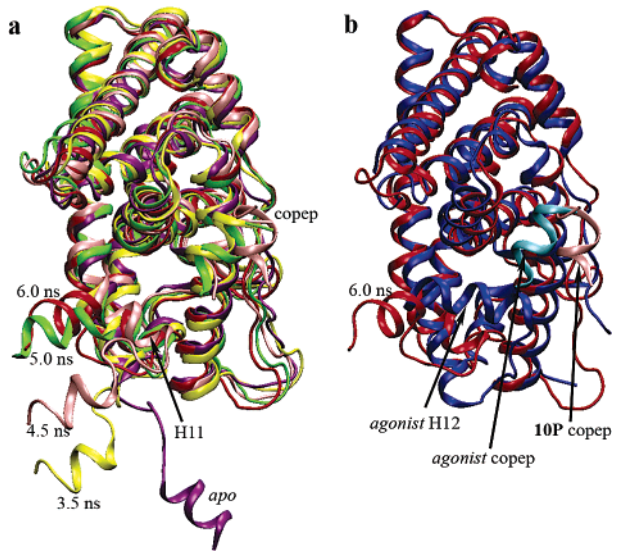

FIGURE 12: (a) Trajectory of model **10P**, including the initial conformation (magenta) and snapshots taken at 3.5 ns (yellow), 4.5 ns (pink), 5.0 ns (green), and 6.0 ns (red). (b) The 6.0 ns snapshot (red) superpositioned with the agonist X-ray structure (blue). The copep is shown in cyan for the agonist structure and in pink in **10P**. H12 is approaching the agonist position after 6 ns, while the copep is tilted out of the site to possibly allow H12 to be positioned.

how many snapshots preserve the hydrogen bonds in the zipper (Supporting Information). An increase in these accumulated numbers cannot be traced after the first nanosecond of the simulation. During the conformational change, H11 is partially unwinding and during the last nanosecond of the simulation, the copep, which is only held in place by half of the "charge clamp" (Lys362), is tilted out to allow for H12 to enter and form the complete co-activator binding site. The two neutral tautomers of His524, models **10D** and **10E**, do not lead to stable conformations of hERα. The behavior observed in **10P**, contrary to that of the other apo models, leads us to conclude that the shift from apo to agonist conformation may happen before a ligand is bound but with a copep coordinated. It is possible that the copep can serve to pull H12 in place.

CONCLUSIONS

In this article, we present an exhaustive, 158 ns non-restrained all-atom molecular dynamics simulation of the hERα LBD to elucidate the binding of the natural ligand E2 and to gain further insight into the dramatic conformational changes governing this protein from its inactive structure to the biologically active form. From the simulations, we conclude that E2 binding in the active form of hERα LBD is favored with the neutral ϵ-tautomer of His524 (model **1**). This tautomer is able to preserve a conserved hydrogen bond from His524 to the substrate and also maintain a hydrogen bond network from His524 to Glu339 (H3) via Glu419 and Lys531 (H11) throughout the simulation. By conserving this network, H3 and H11 are kept in close contact, presumably preventing the ligand from escaping the ligand binding cavity. Furthermore, this network ensures that H12 is positioned in the "mouse trap" because it cannot reach the other favorable (antagonist) position on the hERα LBD surface when H11 is not allowed to unwind. The positioning of H12 then sets up the "charge clamp" that binds a co-activator peptide with a LXXLL motif, leading to the transcriptionally active tertiary complex. From simulations of agonist hERα LBD (model **2**), it is proposed that once the ligand is positioned correctly, the overall structure of the binary agonist hERα LBD complex is stable. Once H12 is positioned in the agonist position in the "mouse trap", it does not move away again whether or not the copep stays bound. A similar simulation at an elevated temperature could further elucidate the most flexible parts of this complex. Thus, it is possible that if the LBD is found in the cell as agonistic holo hERα with bound E2, then diffusing co-activator proteins can associate with this binary complex. We speculate that if other small molecules are present in the cellular environment, then they may be capable of binding in the co-activator binding cleft between H3, H4, and H12, thereby interfering with the transcriptional machinery at this stage of the cycle by inhibiting co-activator binding. Some inhibitors of ER activity have indeed been designed to bind in this site (*86*, *87*). Ongoing research in our group will investigate the possibility for EDCs to bind in this cavity as well as to the alternative ligand binding cavity (*35*, *88*). Simulations of models **3** and **4** of hERα LBD in the agonist conformation without E2 revealed stable proteins on the examined time scale. Specifically, H12 is stable and stays tightly bound to the core of the LBD, and no signs of a conformational change toward an apo or antagonist structure could be detected.

The observation that the hydrogen bond network between E2, His524, Glu419, Lys531 and Glu339 is not intact in the antagonist simulations strongly indicates that His524 must serve a pivotal role in maintaining the local environment between H3 and H11. We suggest that hERα is working by having such a communication link between the presence of an agonist ligand and the overall fold of the LBD of the protein, providing a possible mechanism for the observed allosteric activation within the ligand binding domain of ER. The former is signalled by the presence of a hydrogen bond from the ligand to His524, serving to keep this residue in

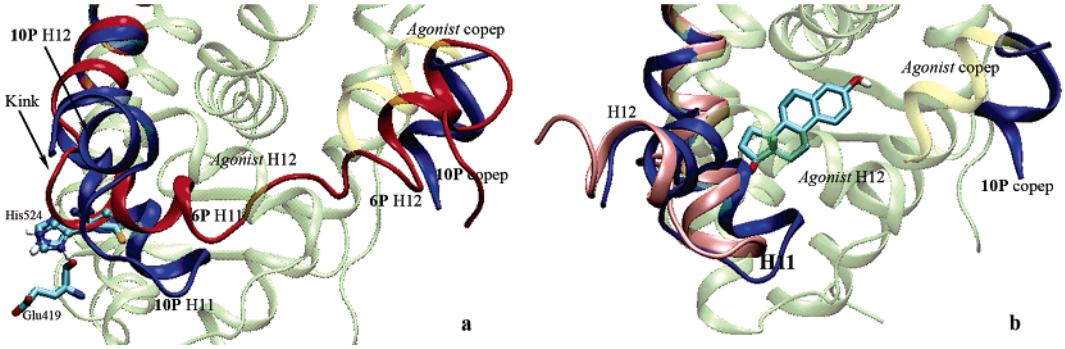

FIGURE 13: Overlay of the agonist X-ray structure (transparent green; copep, transparent yellow) (*21*) with snapshots from (a) **6P** (5 ns; red) and **10P** (6 ns; blue). His524 from **6P** (ball and stick) and **10P** (licorice) is depicted as well as Glu419 from **10P**. (b) **7E** (8.0 ns; pink) and **10P** (6 ns; blue).

position, whereas the latter is signalled by the position of H12. When a hydrogen bond from the ligand to His524 is present, H12 can only rest in the "mouse trap" because His524 is holding in place the hydrogen bond network, serving as the spring of the "mouse trap", which prevents H3 and H11 from un-zipping and thereby providing more flexibility to the positioning of H12. If the bound ligand is not capable of hydrogen bonding to His524, the conserved hydrogen bond network can be disrupted, which then leads to the flexibility observed in the positioning of H12 and to the opening of the binding cavity, allowing for more easy exchange of ligands. Another way to interrupt the hydrogen-bonding network is to remove the Nϵ hydrogen atom on His524. Without this atom, His524 and Glu419 will be repelled, and consequently, the network is disrupted. A His524Ala mutation of hERα LBD in the interaction with various EDCs points in the same direction (*51*) because the differential response seen for the ERα wild type was eliminated by this site point mutation pointing toward His524, having an essential role in the overall conformational dynamic picture of the protein. Model **4** revealed that the presence of a copep in the "charge clamp" can be communicated to the ligand binding cavity by zipping the hydrogen bond network only if His524 is neutral and found in the ϵ-tautomer.

Three of the most dynamic models studied were the antagonist conformation at 400 K, the apo conformation with E2 in the binding site, and the apo conformation with an empty binding site but including the copep, models **6P**, **7E**, and **10P**. The end structures from simulations **6P** and **10P** and a snapshot from simulation **7E** at 8.0 ns are highly similar. RMSDs for all Cα-atoms equal less than 3 Å between the two latter structures. Low RMSDs, below 2.7 Å, are also calculated between model **6P** and models **10P** and **7E** when H12 is excluded. **6P** and **10P** both have His524 modeled with the charged imidazolium ion, whereas **7E** includes the Nϵ-tautomer of the neutral residue. In both of the setups with a charged His524, we observe the formation of a kink between H10 and H11 as well as a partial release of the component (copep or H12) bound in the "charge clamp". A close-up view of the final structures from the two simulations along with the agonist X-ray structure is depicted in Figure 13. Although the two conformations are, of course, not entirely identical, the similarities are easily seen. The C-terminal H12 of **6P** and the copep in **10P** are both partially held in place by hydrogen bonds to Glu362, whereas the N-terminals show more flexibility. For the **6P** simulation, it seems the displacement of H12 serves to pull H11 into the kinked position. Because of this conformational change, His524 is now positioned outside of the binding site, and is surface exposed, hereby opening an entrance to the binding site between H3 and H11. Interestingly, a similar conformation of His524 is observed in **10P**, which was initiated from the apo conformation of the protein. Here, the kink between H10 and H11 is observed without H12 positioned to pull; instead, it appears to be the reverse, and now H11 is positioned to drag H12 into the "mouse trap", forming the agonist conformation. Remarkably, **6P** and **10P** are the only stable setups identified with His524 modeled as charged, strongly indicating this will only happen when this residue is solvent exposed. Because the kink between H10 and H11 is also only observed in simulations **6P** and **10P**, we anticipate that these two features must be highly correlated. In Figure 13b, a close-up view of **7E**, along with **10P** and the agonist structure, is depicted. It is clear that **7E** (8.0 ns) and **10P** (6.0 ns) are highly similar with respect to the conformation of H11 and H12.

The overall results of the simulations form the basis of a more detailed picture of the dynamic equilibrium of hERα LBD, where two activation pathways seem possible (Scheme 3). We suggest that the initial association of the copep to apo hERα LBD, upper part of Scheme 3, stimulates the movement of H12 toward the agonist position without closing the entrance to the ligand binding cavity between H3 and H11. This most likely happens with a surface exposed positively charged His524 as in model **10P**. Once H12 is in or near the agonist position in the "mouse trap", we suggest that His524 becomes deprotonated at Nδ either by the solvent or by a neighboring acidic residue, for example, Glu419. It is possible that E2 enters first and then, by forming a hydrogen bond from E2(O17) to His524(Nδ), pulls His524 inside the cavity, thereby closing the entrance. Further simulations will shed more light on these proposed reaction sequences by examining how the protein can discriminate between the E2 A- and D-rings to orient E2 correctly before entering the binding cavity. Also, we plan to examine if E2(O3) is being guided into the binding cavity by specific interactions. New appropriate setups of the protein with wisely selected protonation states of central residues are needed and in progress in our group.

The other possible pathway involves an initial binding of E2 to the apo conformation of hERα LBD with an ϵ-tautomer of His524 (lower part of Scheme 3). After 7.5−8.0 ns of simulation, a conformational change toward the agonist

Scheme 3 : Two Possible Pathways for the Activation of hERα LBD[a]

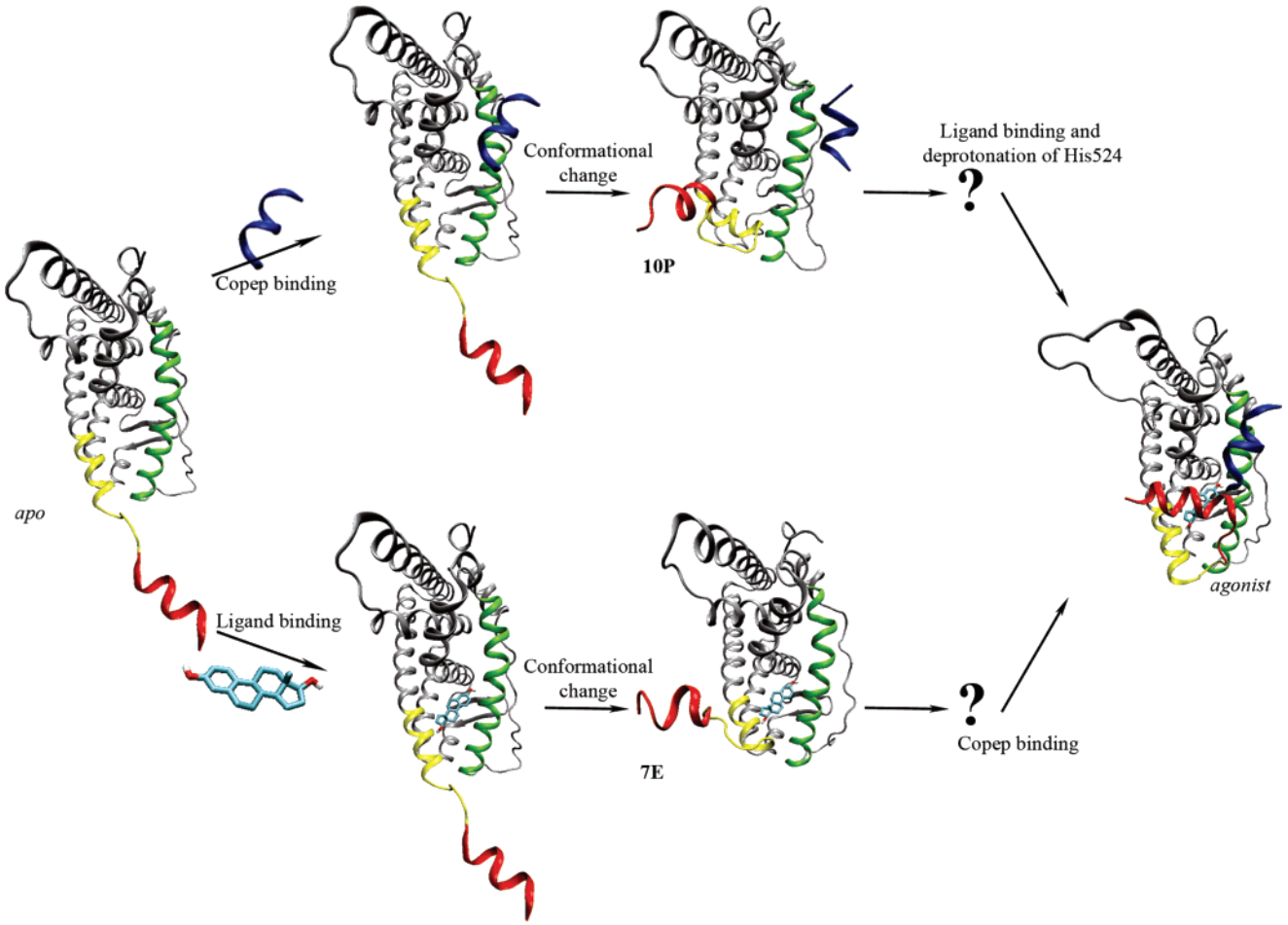

[a] The pathway depends on whether the copep or the ligand is bound first to the apo protein, and there may be a common intermediate before reaching the agonist conformation. The two question marks are included to account for other, yet, undiscovered conformations.

position of H12 is observed. The latter path, though stable on this time scale, may not be as likely because we expect that a charged His524 is more probable when solvent exposed. Further calculations are underway to estimate the energetics associated with the conformational changes. It will be of utmost importance if experimental evidence for the activation of ER can be established with respect to the sequential binding of the two co-factors, E2 and copep. From the simulations, we predict a two-step activation, where the addition of the co-activator peptide is likely to precede the binding of E2, and furthermore, the binding of the first of these co-factors will result in the conformational change before the other co-factor binds.

Moras, Karplus, and co-workers have suggested, from multi ligand copy MD simulations (*53*), that the ligand enters the binding site from the LBD "main entrance" closed by H12 in the agonist conformation. If the same mechanism is found for ER, it will be necessary to un-zip H3 and H11. Our simulations suggest that if the copep binds prior to the ligand, then His524 cannot be present as the Nϵ-tautomer when ligand recognition is taking place because the entrance to the binding cavity is closed in model **4E**. It can, however, proceed if recognition is taking place in a structure similar to that of **10P**, followed by a deprotonation of His524, maybe by nearby residues in the hydrogen bond zipper, Glu419 or Lys531, also giving rise to a zipping of the hydrogen-bonding network. Other pathways have also been studied for RAR and TR (*53*−*57*), and studies are in progress in our group to assess these with respect to our data.

The simulations of the antagonist and agonist structures did not show any signs of an easy conformational change between the two protein conformations in either direction on this time scale, even for miss-matched protein−ligand complexes. We think, that a change from an agonist-to-antagonist fold, or vice versa, is not happening directly; rather, it probably proceeds via an open apo conformation of the hERα LBD. A set of new quasi stable conformations of hERα LBD, models **7D** and **9E**, were identified from the simulations. They are stable for several nanoseconds, which should be enough to be recognized by EDCs or SERMs, thereby disturbing the very delicate conformational equilibrium of ERα LBD. Continuing efforts in our group will look further into this issue.

ACKNOWLEDGMENT

Computations were made possible through allocations of computer time at the PC-Cluster *Horseshoe* at the University of Southern Denmark under the Danish Center for Scientific Computing.

SUPPORTING INFORMATION AVAILABLE

Assignments of the protonation states of histidine residues, residue topology descriptions, added force constants to model estradiol, the RMSD of Cα-atoms for the two remaining

forms of His524, frequencies for hydrogen bond formation in relation to the zipper, helix 11, and the complete citation for the reference on CHARMM (*71*). This material is available free of charge via the Internet at http://pubs.acs.org.

REFERENCES

1. Germain, P., Altucci, L., Bourguet, W., Rochette-Egly, C., and Gronemeyer, H. (2003) Nuclear receptor superfamily: Principles of signaling, *Pure Appl. Chem. 75*, 1619−1664.
2. Nuclear Receptors Nomenclature Committee. (1999) A unified nomenclature system for the nuclear receptor superfamily, *Cell 97*, 161−163.
3. Gronemeyer, H., Gustafsson, J. A., and Laudet, V. (2004) Principles for modulation of the nuclear receptor superfamily, *Nature Rev. Drug Discovery 3*, 950−964.
4. Moore, J. T., Collins, J. L., and Pearce, K. H. (2006) The nuclear receptor superfamily and drug discovery, *ChemMedChem 1*, 504−523.
5. Berkenstam, A., and Gustafsson, J. A. (2005) Nuclear receptors and their relevance to diseases related to lipid metabolism, *Curr. Opin. Pharmacol. 5*, 171−176.
6. Moras, D., and Gronemeyer, H. (1998) The nuclear receptor ligand-binding domain: structure and function, *Curr. Opin. Cell Biol. 10*, 384−391.
7. Bourguet, W., Germain, P., and Gronemeyer, H. (2000) Nuclear receptor ligand-binding domains: three-dimensional structures, molecular interactions and pharmacological implications, *Trends Pharmacol. Sci. 21*, 381−388.
8. Nilsson, S., and Gustafsson, J. A. (2002) Biological role of estrogen and estrogen receptors, *Crit. Rev. Biochem. Mol. Biol. 37*, 1−28.
9. Maglich, J. M., Sluder, A., Guan, X., Shi, Y., McKee, D. D., Carrick, K., Kamdar, K., Wilson, T. M., and Moore, J. T. (2001) Comparison of complete nuclear receptor sets from the human, *Caenorhabditis elegans* and *Drosopila* genomes, *Genome 2*, 00029.1−00029.7.
10. Wrange, Ö, and Gustafsson, J. A. (1978) Separation of the hormone- and DNA-binding sites of the hepatic glucocorticoid receptor by means of proteolysis, *J. Biol. Chem. 253*, 856−865.
11. Wurtz, J. M., Bourguet, W., Renaud, J. P., Vivat, V., Chambon, P., Moras, D., and Gronemeyer, H. (1996) A canonical structure for the ligand-binding domain of nuclear receptors, *Nat. Struct. Biol. 3*, 87−94.
12. Nolte, R. T., Wisely, G. B., Westin, S., Cobbs, J. E., Lambert, M. H., Kurokawa, R., Rosenfeld, M. G., Willson, T. M., Glass, C. K., and Milburn, M. V. (1998) Ligand binding and co-activator assembly of the peroxisome proliferator-activated receptor-γ, *Nature 395*, 137−143.
13. Heery, D. M., Kalkhoven, E., Hoare, S., and Parker, M. G. (1997) A signature motif in transcriptional co-activators mediates binding to nuclear receptors, *Nature 387*, 733−736.
14. Berg, J. M., Tymoczko, J. L., and Stryer, L. (2001) Transcriptional Activation and Repression Are Mediated by Protein-Protein Interactions, *Biochemistry*, 5th ed., pp 879−883, W.H. Freeman and Company, New York.
15. Baniahmad, A. (2005) Nuclear hormone receptor co-repressors, *J. Steroid Biochem. Mol. Biol. 93*, 89−97.
16. Schwabe, J. W. R., Chapman, L., Finch, J. T., Rhodes, D., and Neuhaus, D. (1993) DNA recognition by the oestrogen receptor: from solution to the crystal, *Structure 1*, 187−204.
17. Schwabe, J. W. R., Chapman, L., Fincd, J. T., and Rhodes, D. (1993) The crystal structure of the estrogen receptor DNA-binding domain bound to DNA: How receptors discriminate between their response elements, *Cell 75*, 567−578.
18. Gearhart, M. D., Holmbeck, S. M. A., Evans, R. M., Dyson, H. J., and Wright, P. E. (2003) Monomeric complex of human orphan estrogen related receptor-2 with DNA: A pseudo-dimer interface mediates extended half-site recognition, *J. Mol. Biol. 327*, 819−832.
19. Brozozowski, A. M., Pike, A. C. W., Dauter, Z., Hubbard, R. E., Bonn, T., Engström, O., Öhman, L., Greene, G. L., Gustafsson, J. A., and Carlquist, M. (1997) Molecular basis of agonism and antagonism in the oestrogen receptor, *Nature 389*, 753−757.
20. Tanenbaum, D. M., Wang, Y., Williams, S. P., and Sigler, P. B. (1998) Crystallographic comparison of the estrogen and progesterone receptor's ligand binding domains, *Proc. Natl. Acad. Sci. U.S.A. 95*, 5998−6003.
21. Wärnmark, A., Treuter, E., Gustafsson, J. A., Hubbard, R. E., Brozozowski, A. M., and Pike, A. C. W. (2002) Interaction of transcriptional intermediary factor 2 nuclear receptor box peptides with the coactivator binding site of estrogen receptor α, *J. Biol. Chem. 277*, 21862−21868.
22. Shiau, A. K., Barstad, D., Loria, P. M., Cheng, L., Kushner, P. J., Agard, D. A., and Greene, G. L. (1998) The structural basis of estrogen receptor/coactivator recognition and the antagonism of this interaction by tamoxifen, *Cell 95*, 927−937.
23. Steinmetz, A. C. U., Renaud, J., and Moras, D. (2001) Binding of ligands and activation of transcription by nuclear receptors, *Annu. Rev. Biophys. Biomol. Struct. 30*, 329−359.
24. Egea, P. F., Klaholz, B. P., and Moras, D. (2000) Ligand-protein interactions in nuclear receptors of hormones, *FEBS Lett. 476*, 62−67.
25. Egner, U., Heinrich, N., Ruff, M., Gangloff, M., Mueller-Fahrnow, A., and Wurtz, J. M. (2001) Different ligands-different receptor conformations: Modeling of the hERalpha LBD in complex with agonists and antagonists, *Med. Res. Rev. 21*, 523−539.
26. Bourguet, W., Ruff, M., Chambon, P., Gronemeyer, H., and Moras, D. (1995) Crystal structure of the ligand binding domain of the human nuclear receptor RXRα, *Nature 375*, 377−382.
27. Renaud, J. P., Rochel, N., Ruff, M., Vivat, V., Chambon, P., Gronemeyer, H., and Moras, D. (1995) Crystal structure of the RAR-gamma ligand-binding domain bound to all-trans retinoic acid, *Nature 378*, 681−689.
28. Belleau, B. (1964) Molecular theory of drug action based on induced conformational perturbations of receptors, *J. Med. Chem. 7*, 776−784.
29. Lindorff-Larsen, K., Best, R. B., DePristo, M. A., Dobson, C. M., and Vendruscolo, M. (2005) Simultaneous determination of protein structure and dynamics, *Nature 433*, 128−132.
30. Estabrook, R. A., Luo, J., Purdy, M. M., Sharma, V., Weakliem, P., Bruice, T. C., and Reich, N. O. (2005) Statistical coevolution analysis and molecular dynamics: Identification of amino acid pairs essential for catalysis, *Proc. Natl. Acad. Sci. U.S.A. 102*, 994−999.
31. Agarwal, P. K. (2005) Role of protein dynamics in reaction rate enhancement by enzymes, *J. Am. Chem. Soc. 127*, 15248−15256.
32. Schiøtt, B. (2004) Possible involvement of collective domain movement in the catalytic reaction of soluble epoxide hydrolase, *Int. J. Quantum Chem. 99*, 61−69.
33. Eisenmesser, E. Z., Bosco, D. A., Akke, M., and Kern, D. (2002) Enzyme dynamics during catalysis, *Science 295*, 1520−1523.
34. Gangloff, M., Ruff, M., Eiler, S., Duclaud, S., Wurtz, J. M., and Moras, D. (2001) Crystal structure of a mutant hERα ligand-binding domain reveals key structural features for the mechanism of partial agonism, *J. Biol. Chem. 276*, 15059−15065.
35. Norman, A. W., Mizwicki, M. T., and Norman, D. P. G. (2004) Steroid-hormone rapid actions, membrane receptors and a conformational ensemble model, *Nature Rev. Drug Discovery 3*, 27−41.
36. Shulman, A. I., Larson, C., Mangelsdorf, D. J., and Ranganathan, R. (2004) Structural determinants of allosteric ligand activation in RXR heterodimers, *Cell 116*, 417−429.
37. Nettles, K. W., Sun, J., Radek, J. T., Sheng, S., Rodriguez, A. L., Katzenellenbogen, J. A., Katzenellenbogen, B. S., and Greene, G. L. (2004) Allosteric control of ligand selectivity between estrogen receptors α and β: Implications for other nuclear receptors, *Mol. Cell 13*, 317−327.
38. Yamamoto, K., Abe, D., Yoshimoto, N., Choi, M., Yamagishi, K., Tokiwa, H., Shimizu, M., Makishima, M., and Yamada, S. (2006) Vitamin D receptor: Ligand recognition and allosteric network, *J. Med. Chem. 49*, 1313−1324.
39. Brelivet, Y., Kammerer, S., Rochel, N., Poch, O., and Moras, D. (2004) Signature of the oligomeric behaviour of nuclear receptors at the sequence and structural level, *EMBO Rep. 4*, 423−429.
40. Damstra, T., Barlow, S., Bergman, A., Kavlock, R., and Kraak, G. v. d. (2002) International Programme on Chemical Safety: Global Assessment of the State-of-the-Science of Endocrine Disrupters. World Health Organization.
41. Sumpter, J. P. (1998) Xenoendocrine disrupters-environmental impacts, *Toxicol. Lett. 102*, 337−342.
42. Pillon, A., Boussioux, A. M., Escande, A., Aït-Aïssa, S., Gomez, E., Fenet, H., Ruff, M., Moras, D., Vignon, F., Duchesne, M. J., Casellas, C., Nicolas, J. C., and Balaguer, P. (2005) Binding of estrogenic compounds to recombinant estrogen receptor-alpha: Application to environmental analysis, *Environ. Health Perspect. 113*, 278−284.

43. Colborn, T., vom Saal, F. S., and Soto, A. M. (1993) Developmental effects of endocrine-disrupting chemicals in wildlife and humans, *Environ. Health Perspect. 101*, 378−384.
44. Danzo, B. J. (1997) Environmental xenobiotics may disrupt normal endocrine function by interfering with the binding of physiological ligands to steroid receptors and binding proteins, *Environ. Health Perspect. 105*, 294−301.
45. Sonnenschein, C., and Soto, A. M. (1998) An updated review of environmental estrogen and androgen mimics and antagonists, *J. Steroid Biochem. Mol. Biol. 65*, 143−150.
46. Witorsch, R. J. (2002) Endocrine disrupters: Can biological effects and environmental risks be predicted, *Regul. Toxicol. Pharmacol. 36*, 118−130.
47. Aitken, R. J., Koopman, P., and Lewis, S. E. M. (2004) Seeds of concern, *Nature 432*, 489−52.
48. Jacobs, M. N. (2004) In silico tools to aid risk assessment of endocrine disrupting chemicals, *Toxicology 205*, 43−53.
49. Paige, L. A., Christensen, D. J., Grøn, H., Norris, J. D., Gottlin, E. B., Padilla, K. M., Chang, C. Y., Ballas, L. M., Hamilton, P. T., McDonnell, D. P., and Fowlkes, D. M. (1999) Estrogen receptor (ER) modulators each induce distinct conformational changes in ER alpha and ER beta, *Proc. Natl. Acad. Sci. U.S.A. 96*, 3999−4004.
50. Iannone, M. A., Simmons, C. A., Kadwell, S. H., Svoboda, D. L., Vanderwall, D. E., Deng, S. J., Consler, T. G., Shearin, J., Gray, J. G., and Pearce, K. H. (2004) Correlation between *in vitro* peptide binding profiles and cellular activities for estrogen receptor-modulating compounds, *Mol. Endocrinol. 18*, 1064−1081.
51. Sumbayev, V. V., Bonefeld-Jørgensen, E. C., Wind, T., and Andreasen, P. A. (2005) A novel pesticide-induced conformational state of the oestrogen receptor ligand-binding domain, detected by conformation-specific peptide binding, *FEBS Lett. 579*, 541−548.
52. Shiau, A. K., Barstad, D., Radek, J. T., Meyers, M. J., Nettles, K. W., Katzenellenbogen, B. S., Katzenellenbogen, J. A., Agard, D. A., and Greene, G. L. (2002) Structural characterization of a subtype-selective ligand reveals a novel mode of estrogen receptor antagonism, *Nat. Struct. Biol. 9*, 359−364.
53. Blondel, A., Renaud, J. P., Fischer, S., Moras, D., and Karplus, M. (1999) Retinoic acid receptor: A simulation analysis of retinoic acid binding and the resulting conformational changes, *J. Mol. Biol. 291*, 101−115.
54. Kosztin, D., Izrailev, S., and Schulten, K. (1999) Unbinding of retinoic acid from its receptor studied by steered molecular dynamics. *Biophys. J. 76*, 188−197.
55. Martinez, L., Sonoda, M. T., Webb, P., Baxter, J. D., Skaf, M. S., and Polikarpov, I. (2005) Molecular dynamics simulations reveal multiple pathways of ligand dissociation from thyroid hormone receptors, *Biophys. J. 89*, 2011−2023.
56. Martinez, L., Webb, P., Polikarpov, I., and Skaf, M. S. (2006) Molecular dynamics simulations of ligand dissociation from thyroid hormone receptors: Evidence of the likeliest escape pathway and its implications for the design of novel ligands, *J. Med. Chem. 49*, 23−26.
57. Carlsson, P., Burendahl, S., and Nilsson, L. (2006) Unbinding of retinoic acid from the retinoic acid receptor by random expulsion molecular dynamics, *Biophys. J. 91*, 3151−3161.
58. Adcock, S. A., and McCammon, J. A. (2006) Molecular dynamics: Survey of methods for simulating the activity of proteins, *Chem. Rev. 105*, 1589−1615.
59. Karplus, M., and Kuriyan, J. (2005) Chemical theory and computation special feature: Molecular dynamics and protein function, *Proc. Natl. Acad. Sci. U.S.A. 102*, 6679−6685.
60. Garcia-Viloca, M., Gao, J., Karplus, M., and Truhlar, D. G. (2004) How enzymes work: Analysis by modern rate theory and computer simulations, *Science 303*, 186−195.
61. Benkovic, S. J., and Hammes-Schiffer, S. (2003) A perspective on enzyme catalysis, *Science 301*, 1196−1292.
62. Åqvist, J., and Luzhkov, V. (2000) Ion permeation mechanism of the potassium channel, *Nature 404*, 881−884.
63. Bernéche, S., and Roux, B. (2001) Energetics of ion conduction through the K^+ channel, *Nature 414*, 73−77.
64. de Groot, B. L., and Grubmuller, H. (2005) The dynamics and energetics of water permeation and proton exclusion in aquaporins, *Curr. Opin. Struct. Biol. 15*, 176−183.
65. Forrest, L. R., and Sansom, M. S. (2000) Membrane simulations: bigger and better? *Curr. Opin. Struct. Biol. 10*, 174−181.
66. Saiz, L., and Klein, M. L. (2002) Computer simulation studies of model biological membranes, *Acc. Chem. Res. 35*, 482−489.
67. Hornak, V., Okur, A., Rizzo, R. C., and Simmerling, C. (2006) HIV-1 protease flaps spontaneously open and reclose in molecular dynamics simulations, *Proc. Natl. Acad. Sci. U.S.A. 103*, 915−920.
68. Hornak, V., Okur, A., Rizzo, R. C., and Simmerling, C. (2006) HIV-1 protease flaps spontaneously close to the correct structure in simulations following manual placement of an inhibitor into the open state, *J. Am. Chem. Soc. 128*, 2812−2813.
69. Berman, H. M., Westbrook, J., Feng, Z., Gilliland, G., Bhat, T. N., Weissig, H., Shindyalov, I. N., and Bourne, P. E. (2000) The protein data bank, *Nucleic. Acids Res. 28*, 235−242.
70. Kalé, L., Skeel, R., Bhandakar, M., Brunner, R., Gursoy, A., Krawetz, N., Phillips, J., Shinozaki, A., Varadarajan, K., and Schulten, K. (1999) NAMD2: Greater scalability for parallel molecular dynamics, *J. Comput. Phys. 151*, 283−312.
71. MacKerell, A. D. J., et al. (1998) All-atom empirical potential for molecular modeling and dynamics studies of proteins, *J. Phys. Chem. B 102*, 3586−3616.
72. Jorgensen, W. L., Chandrasekhar, J., Madura, J. D., Impey, R. W., and Klein, M. L. (1983) Comparison of simple potential functions for simulating liquid water, *J. Chem. Phys. 79*, 926−935.
73. Pitman, M. C., Suits, F., MacKerell, A. D. J., and Feller, S. E. (2004) Molecular-level organization of saturated and polyunsaturated fatty acids in a phosphatidylcholine bilayer containing cholesterol, *Biochemistry 43*, 15318−15328.
74. *Accelrys* (2000) Quanta 2000, San Diego, CA.
75. Gilson, M. K., Gilson, H. S. R., and Potter, M. J. (2003) Fast assignment of accurate partial atomic charges. An electronegativity equalization method that accounts for alternate resonance forms, *J. Chem. Inf. Comput. Sci. 43*, 1982−1997.
76. Darden, T., York, D., and Pedersen, L. (1993) Particle mesh Ewald: An N *log(N) method for Ewald sums in large systems, *J. Chem. Phys. 98*, 10089−10092.
77. Feller, S. E., Zhang, Y., Pastor, R. W., and Brooks, B. R. (1995) Constant pressure molecular dynamics simulation: The Langevin piston method, *J. Chem. Phys. 103*, 4613−4621.
78. Humphrey, W., Dalke, A., and Schulten, K. (1996) VMD: Visual molecular dynamics, *J. Mol. Graphics 14*, 33−38.
79. Barlow, D. J., and Thornton, J. M. (1983) Ion pairs in proteins. *J. Mol. Biol. 168*, 867−885.
80. Eiler, S., Gangloff, M., Duclaud, S., Moras, D., and Ruff, M. (2001) Overexpression, purification, and crystal structure of native ERα LBD, *Protein. Expression Purif. 22*, 165−173.
81. Leduc, A., Trent, J. O., Wittliff, J. L., Bramlett, K. S., Briggs, S. L., Chirgadze, N. Y., Wang, Y., Burris, T. P., and Spatola, A. F. (2003) Helix-stabilized cyclic peptides as selective inhibitors of steroid receptor-coactivator interactions, *Proc. Natl. Acad. Sci. U.S.A. 100*, 11273−11278.
82. Schiøtt, B., and Bruice, T. C. (2002) Reaction mechanism of soluble epoxide hydrolase: Insights from molecular dynamics simulations, *J. Am. Chem. Soc. 124*, 14558−14570.
83. Lie, M. A., Celik, L., Jørgensen, K. A., and Schiøtt, B. (2005) Cofactor activation and substrate binding in pyruvate decarboxylase. Insights into the reaction mechanism from molecular dynamics simulations, *Biochemistry 44*, 14792−14806.
84. Renaud, J., Bischoff, S. F., Buhl, T., Floersheim, P., Fournier, B., Halleux, C., Kallen, J., Keller, H., Schlaeppi, J., and Stark, W. (2003) Estrogen receptor modulators: Identification and structure-activity relationships of potent ERα-selective tetrahydroisoquinoline ligands, *J. Med. Chem. 46*, 2945−2957.
85. Kim, S., Wu, J. Y., Birzin, E. T., Frisch, K., Chan, W., Pai, L., Yang, Y. T., Mosley, R. T., Fitzgerald, P. M. D., Sharma, N., Dahllund, J., Thorsell, A., DiNinno, F., Rohrer, S. P., Schaeffer, J. M., and Hammond, M. L. (2004) Estrogen receptor ligands. II. Discovery of benzoxathiins as potent, selecive estrogen receptor α modulators, *J. Med. Chem. 47*, 2171−2175.
86. Schulman, I. G., and Heyman, R. A. (2004) The flip side: Identifying small molecule regulators of nuclear receptors, *Chem. Biol. 11*, 639−646.
87. Rodriguez, A. L., Tamrazi, A., Collins, M. L., and Katzenellenbogen, J. A. (2004) Design, synthesis, and in vitro biological evaluation of small molecule inhibitors of estrogen receptor alpha coactivator binding, *J. Med. Chem. 47*, 600−611.

88. Mizwicki, M. T., Keidel, D., Bula, C. M., Bishop, J. E., Zanello, L. P., Wurtz, J., Moras, D., and Norman, A. W. (2004) Identification of an alternative ligand-binding pocket in the nuclear vitamin D receptor and its functional importance in 1α,25(OH)2-vitamin D3 signalling, *Proc. Natl. Acad. Sci. U.S.A. 101*, 12876−12881.
BI061656T